Nonergodicity in DRADA deuteron glass

Authors: V. Hugo Schmidt & Nicholas J. Pinto

V. Hugo Schmidt & Nicholas J. Pinto (1994) Nonergodicity in drada deuteron glass, Ferroelectrics, 151:1, 257-262, DOI: 10.1080/00150199408244748

NONERGODICITY IN DRADA DEUTERON GLASS

V. HUGO SCHMIDT and NICHOLAS J. PINTO*
Physics Department, Montana State University, Bozeman, MT 59717, USA
*Now at Physics Department, Wichita State University, Wichita, KS 67208

(Received August 9, 1993; in final form October 31, 1993)

Abstract A field-heating (FH), field-cooling (FC), zero-field heating (ZFH) sequence was used to study nonergodic polarization response to dc electric field in x=0.28 $Rb_{1-x}(ND_4)_xD_2AsO_4$ (DRADA) deuteron glass. Polarization change in the low-temperature nonergodic region varied with temperature T nearly as T^y, where $5 \leq y \leq 6$. This result is compared with predictions of the bound charge semiconductor model for proton glass.

INTRODUCTION

For people with a ferroelectrics background, a proton glass like $Rb_{1-x}(NH_4)_xH_2AsO_4$ (RADA) is a mixed crystal with ferroelectric (FE) RbH_2AsO_4 and antiferroelectric (AFE) $NH_4H_2AsO_4$ parent materials. Over a range of about $0.16<x<0.40$ the FE and AFE interactions are frustrated and the crystal exhibits no phase transition.[1,2] Outside this range, both normal[3,4] and deuterated[4] RADA crystals exhibit coexistence of proton glass and ordered FE or AFE phases before the x=0 (FE) and x=1 (AFE) pure phases are reached. For people with a magnetic spin glass background, proton glass is a pseudospin glass with frustrated electric instead of magnetic interactions. The pseudospin's ±1 spin value depends on whether the H atom's off-center position in the O-H···O bond contributes a + or - dipole moment. There are additional differences from spin glasses. First, proton glass interactions are short-range FE and AFE pseudospin-pseudospin interactions[5-9] instead of intermediate-range magnetic spin-spin interactions. Second, spin glasses usually lack significant spin-lattice interactions, but proton glass pseudospins because of their unlike (Rb^+ and NH_4^+) cation neighbors feel a significant bias which eliminates any permittivity cusp,[10] whereas a permeability cusp corresponding to the spin glass "transition" is seen in spin glasses.[11]

Both proton glasses and spin glasses develop with decreasing temperature a large spread in permittivity (permeability) time constants.[12] Below some temperature corresponding to the onset of nonergodicity, the upper time constant limit becomes infinite or at least longer than the experimenter is willing to wait. In the nonergodic state, the crystal cannot reach a new state of minimum free energy

required by changing external conditions (temperature, field, pressure, etc.). To try to observe the onset of nonergodicity, dielectric permittivity techniques can be pushed down to the millihertz or even upper microhertz range, but such experiments are quite time-consuming. One can attempt to observe long polarization decays directly with an electrometer, but leakage and drift cause serious problems.

Levstik et al.[13] circumvented these difficulties by applying to $Rb_{1-x}(NH_4)_xH_2PO_4$ (RADP) a field cooling (FC) technique, to be described later, in which the onset and decay of nonergodicity can be clearly observed. We report here on a modified FC technique applied to RADA, and on an analysis of the results. The motivation for both experiments was investigation of the nature of nonergodicity, including the question of whether there is a well-defined temperature at which the upper time constant limit suddenly becomes infinite, or whether that upper limit increases continuously and only becomes infinite at 0 K.

EXPERIMENTAL METHOD

The crystal was grown by slow evaporation from an aqueous solution of the parent crystals RbD_2AsO_4 and $ND_4D_2AsO_4$ by Z. Trybula. A sample 0.58 mm thick perpendicular to the a axis was cut from the crystal, polished and then electroded with evaporated silver contacts. The crystal was in series with a (much larger capacitance) 15 nF low-leakage capacitor connected across the input of a Model 610R Keithley electrometer, whose voltage was thus proportional to the sample polarization. An Oxford Model ESR-900 continuous-flow liquid-helium cryostat provided and controlled the low temperatures, but temperature was measured independently of this system, with a chromel-alumel Type K thermocouple.

Our temperature and field control cycle consisted in four steps or processes, as described in the following Section together with the experimental results.

EXPERIMENTAL RESULTS

Our technique consisted in first cooling the crystal from room temperature at zero field, so of course no polarization developed and nothing interesting happened in this first step. Then at the lowest temperature of 10 K, we began the field heating (FH) process by suddenly applied a dc field near 800 V/cm along the a axis and started raising the temperature at one of two rates, 1 K/min or 4 K/min. No noticeable rate dependence was seen in our results; with hindsight we should have used a much larger rate ratio because the time dependence of polarization is very weak compared to the temperature dependence in this type of experiment. Results for the 1 K/min run appear in Fig. 1; results for the 4 K/min run as well as both a- and c-axis ac dielectric results will appear elsewhere.[14] The 4 K/min results show that the field application generated an immediate response from the electronic and direct ionic displacements. ("Direct" means not mediated by any hydrogen intrabond motion.) Following this direct response, no further increase occurred until the temperature rose to about 20 K, at which point there was an increase that

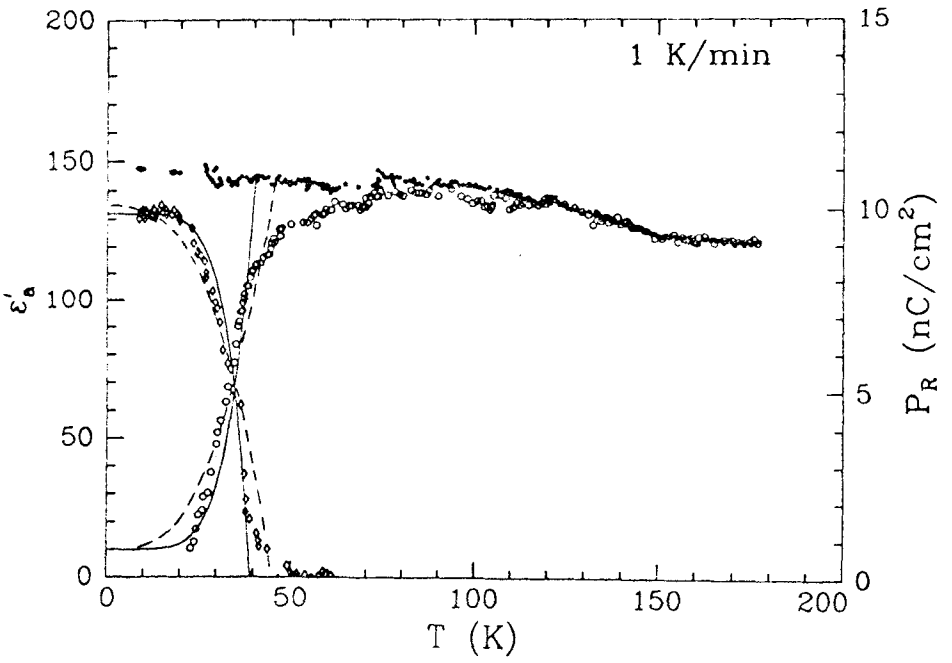

FIGURE 1 Temperature dependence of polarization, and of permittivity in ergodic range, along a axis of x=0.28 DRADA. Open and filled circles and open diamonds indicate field heating, field cooling, and zero field heating results respectively. Solid and dashed lines show fits to polarization change proportional to T^6 and T^3 respectively.

became faster and faster until it approached the value required for minimum free energy, at which point the response flattened out more or less exponentially. The 1 K/min results in Fig. 1 are similar, except that data-taking only began at 22 K, so the flat initial portion found in the 4 K/min run is missing. The temperature was raised further at the same 1 K/min rate after the polarization curve flattened out, stopping near 180 K which is the limit required to prevent ionic (protonic)[15,16] conductivity from causing the electrometer voltage to drift upward.

In the third step, the field cooling (FC) process, the rate of temperature increase was immediately changed to the same 1 K/min rate of temperature decrease, keeping the applied field unchanged at 800 V/cm. In the ergodic regime the polarization retraced the FH curve, increasing according to a Curie-Weiss law and then deviating below the extrapolated Curie-Weiss curve as is typical for proton glasses. Near 60 K (the ergodic limit for this heating/cooling rate) the FC curve separates from the FH curve, the polarization can no longer respond appreciably, and the curve becomes flat as the lowest temperature of 10 K is approached.

At this lowest temperature the last, zero-field heating (ZFH), step is begun by removing the applied field and heating at the same rate as in the FH step. The polarization immediately drops by the amount of the electronic and direct ionic response, then stays unchanged until near 20 K it begins dropping, slowly at first

and then more rapidly, but finally approaches zero more or less exponentially. The ZFH and FH curves are seen to be nearly mirror images of each other.

ANALYSIS

We analyze our results based on ideas related to the bound charge semiconductor model for dielectric response of proton glass.[17] As a simplest illustration of that model, consider RDA in the framework of the Slater-Takagi model[18,19] with dynamics provided by the effective diffusion of $HAsO_4$ and H_3AsO_4 "bound charge carriers" by means of successive hydrogen intrabond transfers, a process first deduced from NMR relaxation results.[20,21] These transfers can convert zero-energy polar Slater groups into nonpolar groups of energy ε_0 and vice versa, or in other words, phonon energy is converted into Slater group configurational energy and vice versa. In equilibrium, the diffusion (hydrogen transfers) should on the average not change the configurational energy, so the diffusion occurs along a path which is level on the average. In proton glass, one must also consider AFE and random bias interactions, but the basic premise of a level path average remains unchanged. If configurational energy is plotted vertically against number of diffusion steps horizontally, one obtains a random walk plot of energy against step number, similar to the well-known "drunkard's walk" plot of position vs. step number. The maximum barrier encountered in diffusing N net steps (in a given sense along the path, without retracing and ignoring side trips) will be proportional to $N^{1/2}$. The maximum barrier that can be crossed (in, say, one minute during which T changes appreciably) will be proportional to temperature T. This means that in this time the number of steps diffused will be proportional to T^2. This diffusion then occurs over a "volume" of size about N^3, proportional to T^6. In the ZFH process one could think of this diffusion as destroying the polarization throughout the diffusion region, so the amount of polarization drop from its initial value should be proportional to T^6. We see in Fig. 1 that the fit to this T^6 law is surprisingly good. Similar arguments can be applied to the polarization rise in the FH process, and the fit is similarly good.

We applied this T^6 "law" to the ZFH data of Levstik et al.[13] for RADP and obtained equally good fit.[14] Their method had no FH process. Instead, they employed what they called a zero-field cooling process and observed the equivalent of the high-temperature end of our FH curve. Their curve extended down to a temperature only slightly below the separation point from their FC curve, so it was not possible to try to fit this curve to the T^6 law.

It is tempting to end the story here and to be proud of our good fit. However, a more careful analysis must take more details of the bound charge semiconductor model into account. For instance, the number of diffusion steps of an $HAsO_4$ or H_3AsO_4 bound charge carrier is not proportional to the radius diffused in real space, because the diffusion path itself is a thermally activated random walk in real space. We then must consider whether the maximum barrier height encountered depends on real space radius or on diffusion path "radius." At the low temperatures for which nonergodicity occurs, the carrier is confined to a small region and its path will include sections that retrace and thus do not change the configurational energy, so we consider that the pertinent radius is the real space

radius. Also, the FH and ZFH processes involve time as well as temperature, and an accurate analysis must include time also as a parameter. We take these considerations into account in the following simple model, which leads to a T^3 law for the polarization decay or rise.

The polarization change in the FH and ZFH processes is the carrier concentration n multiplied by the mean carrier displacement <x> and carrier effective charge q. In the nonergodic regime n is temperature-independent because the carriers are trapped and cannot find annihilation partners. We assume the mean carrier energy relative to the trap site is $\varepsilon_d(r/r_1)^{1/2}$. The 1/2 exponent gives the energy barrier height spatial dependence discussed above and provides the temperature/time limitation on carrier diffusion. ε_d is the rms energy change per path step, and r_1 is the length of one path step. The electrical energy of a carrier is $-qEx=-qEr\cos\theta$, where E is the electric field strength and θ is the polar angle of the carrier relative to the field direction. Integration over r and solid angle yields

$$\Delta P=nq\langle x\rangle=(9!/5!)qE(kT)^3r_1^2/3\varepsilon_d^4=1008qE(kT)^3r_1^2/\varepsilon_d^4 \qquad (1)$$

From the T^3-law fit in Fig. 1, the polarization change equals the initial polarization of 10 nC/cm^2 for the ZFH curve at the "ergodic temperature" T_e=44 K. For r_1 we use 3.24 Å, for q we use the c-axis value[17] of 0.08 proton charge, and we assume a fractional carrier concentration of 0.001, a typical low-temperature value from Monte Carlo simulations. Then Eq. (1) will balance if the rms energy ε_d is chosen as 26 K in temperature units. This is lower than expected by about a factor of 3. Another problem with this simple model is that, as seen in Fig. 1, the data could fit a T^5 law, but one cannot force the exponent much lower. It is puzzling that the T^6 law which is based on naive ideas gives a better fit than the T^3 law based on what seems a more physically sound model.

DISCUSSION

The "nonergodic" type experiments such as the FH and ZFH runs reported here and elsewhere provide a different type of test for any theory of proton glass dynamics than is provided by fits to ac dielectric permittivity data, NMR or Brillouin scattering results, etc. Variations of these nonergodic experiments should be made, for instance using a much broader range of heating/cooling rates, and interrupting FH or ZFH runs by removing or applying a field, respectively, as well as employing different field strengths. A successful theory must be able to explain both the nonergodic and permittivity type experimental data, and it must be based on well-defined local interactions rather than having merely a phenomenological basis. Providing such a theory remains a difficult and exciting challenge.

ACKNOWLEDGEMENTS

This work was supported by NSF Grant DMR-9017429. Dr. Stuart Hutton automated the apparatus used in this experiment. Prof. John Drumheller kindly allowed use of his EPR liquid helium cryostat and temperature control apparatus.

REFERENCES

1. Z. Trybula, J. Stankowski, and R. Blinc, Ferroelectrics Lett. 6, 57 (1986).
2. Z. Trybula, V. H. Schmidt, J. E. Drumheller, D. He, and Z. Li, Phys. Rev. B, 40, 5289 (1989).
3. Z. Trybula, V. H. Schmidt, and J. E. Drumheller, Phys. Rev. B, 43, 1287 (1991).
4. F. L. Howell, N. J. Pinto, and V. H. Schmidt, Phys. Rev. B, 46, 13762 (1992).
5. V. H. Schmidt, S. Waplak, S. Hutton, and P. Schnackenberg, Phys. Rev. B, 30, 2795 (1984).
6. E. Matsushita and T. Matsubara, Prog. Theor. Phys., 71, 235 (1984).
7. Y. Ishibashi and I. Suzuki, J. Phys. Soc. Jpn., 54, 1443 (1985).
8. V. H. Schmidt, J. T. Wang, and P. Schnackenberg, Jpn. J. Appl. Phys., 24, Suppl. 24-2, 944 (1985).
9. V. H. Schmidt, Ferroelectrics, 72, 157 (1987).
10. R. Pirc, B. Tadić, and R. Blinc, Phys. Rev. B, 36, 8607 (1987).
11. G. Parisi, J. Phys. A, 13, 1101 (1980).
12. E. Courtens, Phys. Rev. Lett., 52, 69 (1984).
13. A. Levstik, C. Filipič, Z. Kutnjak, I. Levstik, R. Pirc, B. Tadić, and R. Blinc, Phys. Rev. Lett., 66, 2368 (1991).
14. N. J. Pinto, K. Ravindran, and V. H. Schmidt, to appear in Phys. Rev. B.
15. V. H. Schmidt, J. Sci. Instrum., 42, 889 (1965).
16. L. Glasser, Chem. Rev., 75, 21 (1975).
17. V. H. Schmidt, Ferroelectrics, 78, 407 (1988).
18. J. C. Slater, J. Chem. Phys. 9, 16 (1941).
19. Y. Takagi, J. Phys. Soc. Jpn., 3, 273 (1948).
20. V. H. Schmidt and E. A. Uehling, Phys. Rev., 126, 447 (1962).
21. V. H. Schmidt, Phys. Rev., 164, 749 (1967).